Conformational Distribution of Tetramethoxycalix[4]arenes by Molecular Modeling and NMR Spectroscopy: A Study of Apolar Solvation

Willem P. van Hoorn,[†] Wim J. Briels,[‡] John P. M. van Duynhoven,[§] Frank C. J. M. van Veggel,[†] and David N. Reinhoudt*,[†]

Laboratories of SupraMolecular Chemistry and Technology, Chemical Physics, and Chemical Analysis, University of Twente, P.O. Box 217, 7500 AE Enschede, The Netherlands

Received November 21, 1997

The influence of the solvents dichloromethane and chloroform on the conformational distribution of a tetramethoxycalix[4]arene **2b** (R = t-Bu) has been investigated by ^{1}H NMR and molecular modeling with the CHARMM force field. This calix[4]arene derivative can exist in the cone, partial cone, 1,2-alternate, and 1,3-alternate conformations. The cone/partial cone equilibrium showed the largest solvent effect during measurements in CD_2Cl_2 and $CDCl_3$. The conformational distribution of **2b** was calculated in a vacuum with the Boltzmann equation based on the sum of the minimized potential energies and the vibrational and rotational free energies. The influence of the solvent was investigated by molecular dynamics simulations. These simulations show that the cavity of the cone of **2b** contains a solvent molecule in dichloromethane, but not in chloroform. Although the inclusion of a chloroform molecule is enthalpically favorable, it is not stable because of the unfavorable entropy of complex formation. In both chloroform and dichloromethane, one conformer (0001∼AAAB) is the most stable Paco; in this conformation the methoxy moiety connected to the inverted aromatic ring is pointing into the cavity of **2b**. The increased stability of this conformer is due to the possibility to form CH··O hydrogen bonds.

Introduction

Calix[4]arenes are macrocyclic compounds which are increasingly being used as building blocks in supramolecular chemistry.[1,2] One interesting property of calix[4]arenes is that they can exist in four extreme conformations (Chart 1), designated the cone, the partial cone (Paco), the 1,2-alternate (1,2Alt), and the 1,3-alternate (1,3Alt).

The cone conformation has a cavity which has inspired the use of calix[4]arenes as host molecules and potential enzyme mimics.[3] Tetrahydroxycalix[4]arenes **1** adopt the cone conformation in chloroform solution due to a circular array of hydrogen bonds.[4] The tetramethyl derivatives **2** cannot form internal hydrogen bonds which favor the cone conformation, and multiple conformations of **2b** (R = *t*-Bu) are found by NMR spectroscopy in $CDCl_3$ (Table 1).[5−9] The four conformations of **2b** interconvert rapidly with the Paco as the key intermediate.[9,10]

The conformational behavior, the simplicity of the molecule, and the large number of experimental studies available from the literature render calix[4]arenes ideal model systems for testing computational methodology. Several studies have been published[6−9,11,12] in which the relative stabilities of the conformations of **2b** have been calculated using force field and semiempirical energy minimizations.[13] None of these studies could reproduce the experimental relative abundances of the four conformations of **2b**. To illustrate this point, we have calculated the Boltzmann distribution from the published minimized energies and compared them to experimental results (Table 1). Of the 14 published energy minimizations of **2b**, only 7 succeeded in determining the most stable conformation (Paco), but 6 found the experimen-

[†] SupraMolecular Chemistry and Technology.
[‡] Chemical Physics.
[§] Chemical Analysis.

(1) (a) Gutsche, C. D. *Calixarenes*; Royal Society of Chemistry: Cambridge, 1989. (b) *Calixarenes; A Versatile Class of Compounds*; Vicens, J., Böhmer, V., Eds.; Kluwer Academic Publishers: Dordrecht, 1991. (c) Böhmer, V. *Angew. Chem., Int. Ed. Engl.* **1995**, *34*, 713−745. (d) Pochini, A.; Ungaro, R. *Comprehensive Supramolecular Chemistry*; Vögtle, F., Ed.; Pergamon Press: 1996; Vol 2, pp 103−142.

(2) (a) Timmerman, P.; Verboom, W.; van Veggel, F. C. J. M.; van Hoorn, W. P.; Reinhoudt, D. N. *Angew. Chem., Int. Ed. Engl.* **1994**, *33*, 1292−1295. (b) Timmerman, P.; Nierop, K. G. A.; Brinks, E. A.; Verboom, W.; van Veggel, F. C. J. M.; van Hoorn, W. P.; Reinhoudt, D. N. *Chem. Eur. J.* **1995**, *1*, 132−143.

(3) (a) Gutsche, C. D.; Dhawan, B.; No, K. H.; Muthukrishnan, R. *J. Am. Chem. Soc.* **1981**, *103*, 3782−3792. (b) Bauer, L. J.; Gutsche, C. D. *J. Am. Chem. Soc.* **1985**, *107*, 6063−6069.

(4) (a) Happel, G.; Mathiasch, B.; Kämmerer, H. *Macromol. Chem.* **1975**, *176*, 3317−3334. (b) Gutsche, C. D.; Bauer, J. *J. Am. Chem. Soc.* **1985**, *107*, 6052−6059. (c) Araki, K.; Shinkai, S.; Matsuda, T. *Chem. Lett.* **1989**, 581−584.

(5) Gutsche, C. D.; Dhawan, B.; Levine, J. A.; No, K. H.; Bauer, L. J. *Tetrahedron* **1983**, *39*, 409−426.

(6) Grootenhuis, P. D. J.; Kollman, P. A.; Groenen, L. C.; Reinhoudt, D. N.; van Hummel, G. J.; Ugozzoli, F.; Andreetti, G. D. *J. Am. Chem. Soc.* **1990**, *112*, 4165−4176.

(7) Iwamoto, K.; Araki, K.; Shinkai, S. *J. Org. Chem.* **1991**, *56*, 4955−4962.

(8) (a) Harada, T.; Rudziǹski, J. M.; Shinkai, S. *J. Chem. Soc., Perkin Trans. 2* **1992**, 2109−2115. (b) Harada, T.; Rudziǹski, J. M.; Osawa, E.; Shinkai, S. *Tetrahedron* **1993**, *49*, 5941−5954.

(9) Groenen, L. C.; van Loon, J.-D.; Verboom, W.; Harkema, S.; Casnati, A.; Ungaro, R.; Pochini, A.; Ugozzoli, F.; Reinhoudt, D. N. *J. Am. Chem. Soc.* **1991**, *113*, 2385−2392.

(10) van Loon, J.-D.; Groenen, L. C.; Wijmenga, S. S.; Verboom, W.; Reinhoudt, D. N. *J. Am. Chem. Soc.* **1991**, *113*, 2378−2384.

(11) Lipkowitz, K. B.; Pearl, G. *J. Org. Chem.* **1993**, *58*, 6729−6736.

(12) Fischer, S.; Grootenhuis, P. D. J.; Groenen, L. C.; van Hoorn, W. P.; van Veggel, F. C. J. M.; Reinhoudt, D. N.; Karplus, M. *J. Am. Chem. Soc.* **1995**, *117*, 1611−1620.

(13) Grant, G. H.; Richards, W. G. *Computational Chemistry*; Oxford University Press: Oxford, 1995.

S0022-3263(97)02134-8 CCC: $15.00
Published on Web 02/03/1998

Table 1. Modeling and Experimental Results on the Conformational Distribution of Tetramethoxycalix[4]arene 2b

	energy (kcal mol^{-1})				Boltzmann distribution (%)[a]				
method	Paco	cone	1,2Alt	1,3Alt	Paco	cone	1,2Alt	1,3Alt	ref
NMR $CDCl_3$					85	4	8	3	9
NMR $CDCl_3$					86	6	6	3	8a
AMBER[c]	0.0	4.6	4.9	−1.8	9	0	0	91	6
MM2[d]	0.0	0.0	3.8	−3.6	0	0	0	100	11
AMBER[d]	0.0	0.0	6.5	−2.5	2	1	0	97	11
OPLSA[d]	0.0	−0.1	9.1	−6.0	0	0	0	100	11
QUANTA 3.3[e]	0.0	76.0	16.3	34.0	100	0	0	0	11
QUANTA 4.0	0.0	−0.9	4.7	3.3	38	62	0	0	this work
MOPAC AM1	0.0	15.8	4.9	4.5	100	0	0	0	11
MOPAC PM3	0.0	14.3	5.5	2.0	100	0	0	0	11
AMPAC AM1	0.0	−2.4	2.2	−25.6	0	0	0	100	11
AMPAC PM3	0.0	−0.6	6.6	5.1	55	45	0	0	11
QUANTA 2.1[f]	0.0	6.0	3.8	1.8	99	0	0	1	9
MM2P	0.0	1.1	4.3	−1.7	10	0	0	90	7
MM3	0.0	1.5	6.1	1.5	98	1	0	1	8a
MM3[b]	0.0	1.5	6.1	1.5	97	2	0	1	8a
CHARMM22[g]					64	0	18	18	12

[a] The Boltzmann distribution is calculated with the following degeneracy numbers: cone: 2; Paco: 8; 1,2Alt: 4; 1,3Alt: 2. These numbers reflect the number of conformations: For the cone: 0000 and 1111; for the Paco: 1000, 0100, 0010, 0001, 0111, 1011, 1101, and 1110; for the 1,2Alt: 1100, 0110, 0011, and 1001; for the 1,3Alt: 1010 and 0101. The digits in the names of the conformations indicate which anisole ring is inverted. For example: 0000 is a cone, 1000 is a Paco, etc. [b] Boltzmann distribution as calculated in ref 8a. This distribution could be reproduced using the following degeneracy numbers: cone: 2; Paco: 4; 1,2Alt: 2; 1,3Alt: 1. [c] As contained in MacroModel 1.5. [d] As contained in MacroModel 3.5. [e] Probably erroneous, compare to entry QUANTA 4.0 (this work) which contains the same parameters as QUANTA 3.3. [f] Two methoxy groups are pointing inward for the 1,2Alt. [g] Based on all in/out positions for the methoxy moieties (28 conformations).

Chart 1. The Four Extreme Conformations of Calix[4]arenes

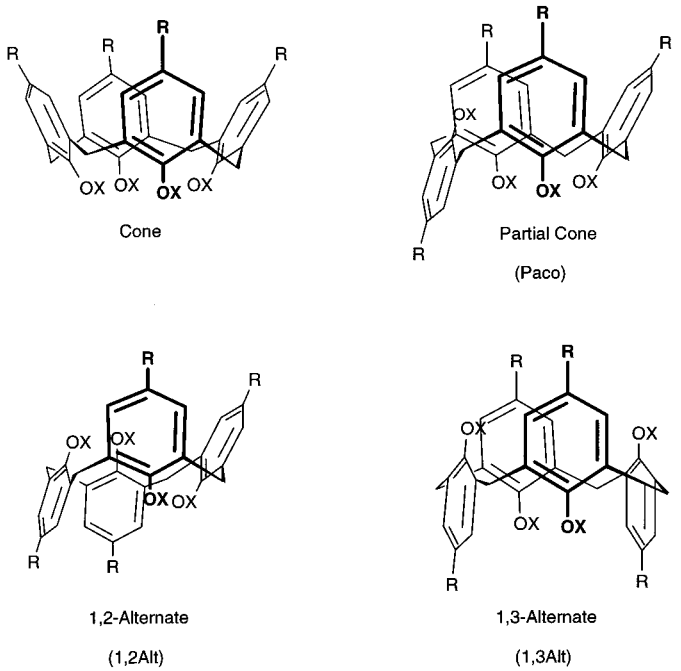

	OX	R
1a	OH	H
1b	OH	t-Bu
2a	OMe	H
2b	OMe	t-Bu
3a	OCO_2Et	t-Bu
3b	OCH_2CO_2Et	t-Bu
3c	OCH_2CONEt_2	t-Bu

tally least stable conformation (1,3Alt) to be present in more than 90% abundance.

In this paper we address the conformational properties of calix[4]arene **2b** *in solution*. The focus is on the question why the experimental conformational distribution of tetramethoxycalix[4]arenes is not correctly reproduced by the published force field calculations. First, we have improved the calculation of the conformational distributions in vacuo, by including the vibrational and rotational degrees of freedom.[14] This provides insight in the differences in internal potential energies and degrees of freedom of the conformations. Second, we have used molecular dynamics (MD) simulations to evaluate the influence of chloroform and dichloromethane on the conformational distributions. Solvents may influence the conformational distribution either by the polarity of the solvent,[15] or by specific inclusion of a solvent molecule in the cavity of the cone.[16] The four conformations of calix[4]arenes have different dipole moments,[15,17] and polar solvents are expected to stabilize the conformation

(14) Hill, T. L. *An Introduction to Statistical Thermodynamics*; Addison-Wesley Publishing Company, Inc.; Reading, 1960.

(15) Iwamoto, K.; Ikeda, A.; Araki, K.; Harada, T.; Shinkai, S. *Tetrahedron* **1993**, *49*, 9937−9946.

(16) Groenen, L. C.; Steinwender, E.; Lutz, B. T. G.; van der Maas, J. H.; Reinhoudt, D. N. *J. Chem. Soc., Perkin Trans 2* **1992**, 1893−1898.

(17) de Mendoza, J.; Prados, P.; Campillo, N.; Nieto, P. M.; Sánchez, C.; Fayet, J.-P.; Vertut, M. C.; Jaime, C.; Elguero, J. *Recl. Trav. Chim. Pays-Bas* **1993**, *112*, 367−369.

with the highest dipole, i.e. the cone.[15] Solvent inclusion in the cone is known from X-ray structures of calix[4]-arenes.[18] The presence of *tert*-butyl moieties at the para position is believed to be essential for the inclusion of solvent molecules; the cavity of calix[4]arenes without para substituents is considered too shallow to contain any guest molecules.[19] A strong indication that inclusion of a solvent molecule is taking place in the liquid state was provided by calorimetric studies of calix[4]arene **3b**.[20] Wipff et al. have performed Molecular Dynamics (MD) simulations of **3c** in vacuo, with a MeCN, MeOH, or water molecule inside the cavity of the cone.[21] All of these included solvent molecules remained encapsulated during a 100 ps simulation, indicating that solvent inclusion is feasible.

Methods

Energy Minimization. Version 23f3 of the CHARMM[22] program was used. Energies of the calix[4]arenes were evaluated with the parameters, partial charges, and energy function described in ref 12. The energy-minimized conformations of **2b** were taken from ref 12. The energies of the conformations were minimized until the root-mean-square value of the energy gradient was less than 10^{-12} kcal mol^{-1} Å^{-1}.

Normal Mode Calculation. All $3N$ (in which N the number of atoms) modes were calculated. Each energy-minimized conformation was checked to be a true minimum by checking the absence of negative frequencies, and the presence of six zero frequencies. The maximum deviation from zero was in the order of ≈0.2 cm^{-1}. The classical (ΔA_{cl}) and quantum mechanical (ΔA_{QM}) vibrational free energies as well as the zero point correction energy (ΔA_0) were calculated[23] with eqs 1−3,

$$\Delta A_{QM} = kT\sum_{i=7}^{3N} \ln(1 - e^{-h\nu_i/kT}) \quad (1)$$

$$\Delta A_{cl} = kT\sum_{i=7}^{3N} \ln\left(\frac{h\nu_i}{kT}\right) \quad (2)$$

$$\Delta A_0 = \sum_{i=7}^{3N} \frac{h\nu_i}{2} \quad (3)$$

in which k is the Boltzmann constant, T the temperature in Kelvin, N the number of atoms, h the constant of Planck, and ν_i the frequency of the ith mode.

Calculation of Rotational Free Energy. The rotational free energy ΔA_{rot} was calculated[14] according to eq 4:

$$\Delta A_{rot} = -kT \ln\left\{\frac{\pi^{1/2}}{\sigma}\left(\frac{T^3}{\Theta_A\Theta_B\Theta_C}\right)^{1/2}\right\} \quad (4)$$

$$\Theta = \left(\frac{h^2}{8\pi^2 Ik}\right) \quad (5)$$

In these equations σ represents the rotational symmetry number, and I one of the three moments of inertia.

Boltzmann Distribution. The probability p of finding a conformation i is given by eq 6:

$$p(i) = \frac{n_i e^{-\Delta A_i/kT}}{\sum_{\text{all } i} n_i e^{-\Delta A_i/kT}} \times 100\% \quad (6)$$

$$\Delta A_i^{QM} = E_{min} + \Delta A_{QM} + \Delta A_0 + \Delta A_{rot}$$
$$\Delta A_i^{cl} = E_{min} + \Delta A_{cl} + \Delta A_{rot} \quad (7)$$

In these equations n_i is the degeneracy of conformation i, and E_{min} the minimized potential energy of i.

Molecular Dynamics Simulation. The OPLS solvent models of Jorgensen[24] were used. The nonbonded interactions were calculated with a list-based cutoff of 14 Å. Full periodic boundary conditions were imposed. A dielectric constant $\epsilon = 1$ was used. The electrostatic interaction was smoothed using the shift function, the van der Waals interaction with a switch function between 11 and 14 Å. The nonbonded lists were updated with a list cutoff of 15 Å with a heuristic test for updating. SHAKE[25] constraints were applied to all bonds with hydrogen atoms, allowing an integration time step of 1 fs. The starting structures for the MD simulations of the cone of **2b** with an included solvent molecule were generated as follows. A C_{4v} cone[12] was minimized in vacuo with the solvent (chloroform or dichloromethane) in the cavity. Complexes with a Cl atom as well as with a CH_x atom in the cavity of **2b** were minimized in vacuo. The two complexes with chloroform were each centered in a 33.0 Å cubic box of 267 chloroform molecules, and the dichloromethane complex was centered in a 30.4 Å cubic box containing 267 dichloromethane molecules. For all MD simulations, the overlapping solvent molecules were removed (*i.e.* any solvent molecule containing an atom within 2.0 Å of any non-hydrogen atom of **2b** was removed). Subsequently, the energy of the solvated complex was minimized. The MD simulation was started with a 5 ps phase in which the system was heated to 300 K, followed by 10 ps equilibration during which velocity scaling was applied if the temperature was outside the 300 ± 10 K window. Finally, a 500 ps (*NVE*) production run was calculated. The temperature did not systematically deviate from 300 K. Coordinates were saved every 200 time steps.

Travel. The Conjugate Peak Refinement (CPR) algorithm[26−28] searches for maxima along the adiabatic energy valley connecting two local minima on an adiabatic energy

(18) (a) Compound **1b** with toluene in the cavity: Andreetti, G. D.; Ungaro, R.; Pochini, A. *J. Chem. Soc., Chem. Commun.* **1979**, 1005−1007. (b) Tetracarbonate derivative **3a** with MeCN in the cavity: McKervey, M. A.; Seward, E. M.; Ferguson, G.; Ruhl, B. L. *J. Org. Chem.* **1986**, *51*, 3581−3584. (c) A 1,3-diethoxy derivative of **1b** with EtOH in the cavity: Bugge, K.-E.; Verboom, W.; Reinhoudt, D. N.; Harkema, S. *Acta Crystallogr., C* **1992**, *48*, 1848−1851. (d) A 1,3 lower rim bridged derivative of **1b** with dichloromethane: Böhmer, V.; Ferguson, G.; Gallagher, J. F.; Lough, A. J.; McKervey, M. A.; Madigan, E.; Moran, M. B.; Phillips, J.; Williams, G. *J. Chem. Soc., Perkin Trans. 1* **1993**, 1521−1527. (e) Alumino bis(*p-tert*-butylcalix[4]arene) with included dichloromethane: Atwood, J. L.; Bott, S. G.; Jones, C.; Raston, C. L. *J. Chem. Soc., Chem. Commun.* **1992**, 1349−1351. (f) The 1,3-bis-*tert*-butyl ester of **1b** with dichloromethane in the cavity: Ferguson, G.; Gallagher, J. F.; Li, Y.; McKervey, M. A.; Madigan, E.; Malone, J. F.; Moran, M. B.; Walker, A. *Supramol. Chem.* **1996**, *7*, 223−228. (g) **1b** with 20 different guests but no chloroform or dichloromethane: Brouwer, E. B.; Enright, G. D.; Ripmeester, J. A. *Supramol. Chem.* **1996**, *7*, 7−9. (h) **1b** with cyclohexane and *n*-pentane: Brouwer, E. B.; Enright, G. D.; Ripmeester, J. A. *Supramol. Chem.* **1996**, *7*, 143−145.

(19) Andreetti, G. D.; Pochini, A.; Ungaro, R. *J. Chem. Soc., Perkin Trans. 2* **1983**, 1773−1779.

(20) Danil de Namor, A. F.; Apaza de Sueros, N.; McKervey, M. A.; Barrett, G.; Arnaud Neu, F.; Schwing-Weill, M. J. *J. Chem. Soc., Chem. Commun.* **1991**, 1546−1548.

(21) Guilbaud, P.; Varnek, A.; Wipff, G. *J. Am. Chem. Soc.* **1993**, *115*, 8298−8312.

(22) Brooks, B. R.; Bruccoleri, R. E.; Olafson, B. D.; States, D. J.; Swaminathan, S.; Karplus, M. *J. Comput. Chem.* **1983**, *4*, 187−217.

(23) Brooks, B. R.; Janežič, D.; Karplus, M. *J. Comput. Chem.* **1995**, *12*, 1522−1542.

(24) $CHCl_3$: Jorgensen, W. L.; Briggs, J. M.; Contreras, M. L. *J. Phys. Chem.* **1990**, *94*, 1683−1686. CH_2Cl_2: Lim, D.; Hrovat, D. A.; Borden, W. T.; Jorgensen, W. L. *J. Am. Chem. Soc.* **1994**, *116*, 3494−3499.

(25) van Gunsteren, W. F.; Berendsen, H. J. C. *Mol. Phys.* **1977**, *34*, 1311−1327.

(26) Fischer, S.; Karplus, M. *Chem. Phys. Lett.* **1992**, *194*, 252−261.

surface. These maxima are refined to saddle points and represent the transition states of the reaction pathway between the two minima. All the degrees of freedom of the molecule can contribute to the reaction path. There is no need to choose a reduced reaction coordinate such as a rotation around a certain bond. The algorithm has been integrated into CHARMM[22] in the travel module.

NMR Spectroscopy. The NMR experiments were performed on a Varian Unity 400WB NMR spectrometer interfaced to a SUN Sparc 10 workstation. The 1D ^{1}H NMR spectra were obtained with relaxation times of $5\times T_1$ in the temperature range 188−303 K. Sample concentrations were 0.02 M. The relative intensities of the ^{1}H NMR signals were obtained by iterative simulation (deconvolution) of the NMR spectrum as a function of Lorentzian line shapes (using the VnmrS/VnmrX package). NOESY/EXSY experiments[29] were performed by using standard Varian pulse programs. Mixing times were typically 100 ms. Thermodynamic parameters with error estimates were obtained from linear interpolation of van't Hoff plots (ln K vs 1/T), where the slope gives $-\Delta H/R$ and the intercept $\Delta S/R$.

Results and Discussion

NMR Spectroscopy. The influence of the solvent on the conformational distribution has been investigated by NMR spectroscopy in both dichloromethane and in chloroform. These solvents were chosen because they differ in dielectric constant[30] (ϵ_r dichloromethane = 9.08, ϵ_r chloroform = 4.81) and dipole moment[30] (dichloromethane = 1.6 D, chloroform = 1.0 D). But more important, X-ray studies have shown that dichloromethane can be included in the cavity of a cone,[18d−f] while the inclusion of chloroform has never been proven.[31−33] The ^{1}H NMR resonances of the respective conformers of **2b** (R = t-Bu) were assigned by means of NOESY/EXSY connectivity patterns and were generally in accordance with available literature data in chloroform.[8a,9] Many of the ^{1}H NMR signals of the respective conformers were overlapping with each other, thus hampering quantitative analysis. The relative abundances of the conformers of **2b** could be accurately obtained by deconvolution of the ^{1}H NMR spectrum in Lorentzian line shapes. For the calculation of the conformational distributions, only the intensities of the methoxy signals were used.

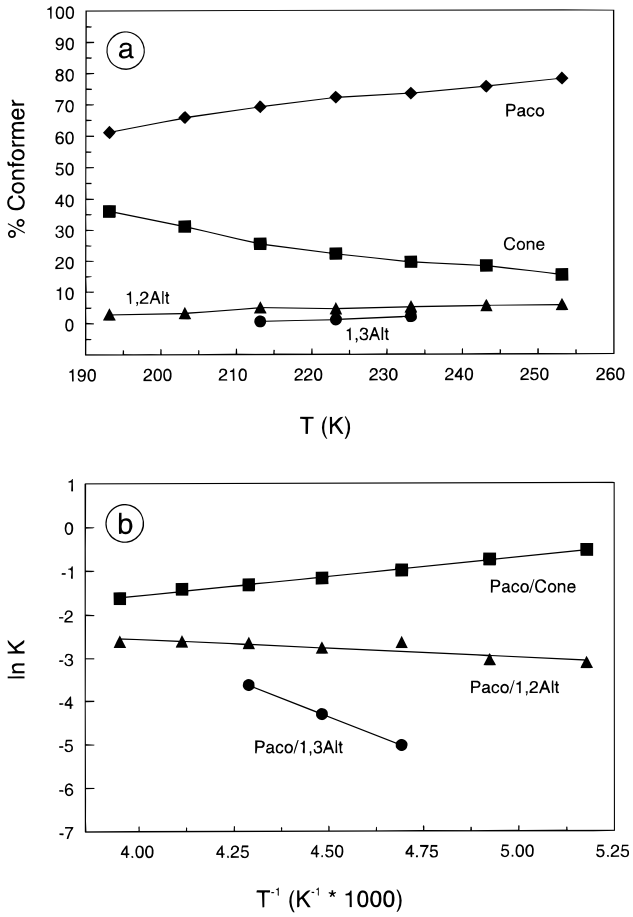

Figure 1. Conformational distribution (a) and van't Hoff plot (b) of **2b** in CD_2Cl_2.

Table 2. Thermodynamic Parameters (kcal mol^{-1}) for the Conformational Equilibrium of 2b in $CDCl_3$ and CD_2Cl_2 As Determined by NMR[a−c]

equilibrium	$\Delta G°$	$\Delta H°$	$T\Delta S°$
in CD_2Cl_2			
Paco/cone	0.7	−1.7 (0.1)	−2.4 (0.02)
Paco/1,2Alt	1.3	0.8 (0.2)	−0.5 (0.06)
Paco/1,3Alt	1.5	*d*	*d*
in $CDCl_3$			
Paco/cone	1.2	1.9 (0.1)	0.7 (0.03)
Paco/1,2Alt	1.3	1.0 (0.1)	−0.4 (0.06)
Paco/1,3Alt	2.2	−0.8 (0.1)	−3.0 (0.12)

[a] Data **2b** in $CDCl_3$ data from ref 8a. [b] $\Delta G°$ and $T\Delta S°$ are given at T = 243 K. [c] In brackets: error determined from least-squares analysis of the van't Hoff plots. [d] No accurate calculation of $\Delta H°$ and $\Delta S°$ possible.

The conformational distribution of **2b** in dichloromethane as function of temperature is presented in Figure 1. This conformational distribution allowed the calculation of a van't Hoff plot, from which the thermodynamic parameters of Table 2 have been derived. The amount of cone present in CD_2Cl_2 is larger than in $CDCl_3$. And the stability of the cone of **2b** as function of temperature is different in both solvents. In CD_2Cl_2 the cone becomes less stable with increasing temperature, while in $CDCl_3$ the cone becomes more stable with increasing temperature. This difference in temperature dependence is expressed in the ΔH and $T\Delta S$ values for the Paco/cone equilibrium in Table 2; for **2b** in CD_2Cl_2

(27) (a) Fischer, S.; Michnick, S.; Karplus, M. *Biochemistry* **1993**, *32*, 13830−13837. (b) Fischer, S.; Dunbrack, R. L., Jr.; Karplus, M. *J. Am. Chem. Soc.* **1994**, *116*, 11931−11937. (c) Verma, C. S.; Fischer, S.; Caves, L. S. D.; Roberts, G. C. K.; Hubbard, R. E. *J. Phys. Chem.* **1996**, *100*, 2510−2518.

(28) van Hoorn, W. P.; van Veggel, F. C. J. M.; Reinhoudt, D. N. *J. Org. Chem.* **1996**, *61*, 7180−7184.

(29) Ernst, R. R.; Bodenhausen, G.; Wokaun, A. *Principles of Nuclear Magnetic Resonance in One and Two Dimensions*; International Series of Monographs on Chemistry, Vol. 14, Breslow, R., Goodenough, J. B., Halpern, J., Rowlinson, J. S., Eds.; Clarendon Press: Oxford, 1987.

(30) *Handbook of Chemistry and Physics*; Weast, R. C., Ed.; The Chemical Rubber Co.: Cleveland, 1971.

(31) A search in the CSD database[32] (May 1997) revealed two calix[4]arenes in the cone conformation with included chloroform. In both cases the cavity of the calix[4]arene is enlarged with respect to simple *p-tert*-butyl derivatives. Delaigue et al.[33a] describe a derivative in which two molecules **1b** are connected at the lower rim via two silicon atoms. The silicon atoms force the lower rim oxygen atoms in close proximity to each other, which enlarges the cavity at the upper rim. Juneja *et al.*[33b] found chloroform inclusion in a *p*-phenyl derivative of **1a**. In this compound, the chloroform is included between these phenyl moieties and not in the cavity of the calix[4]arene itself. Despite many references in the literature to a paper by Gutsche et al.,[3a] we could not find a publication describing chloroform inclusion in either **1b** or tetraalkylated derivates of **1b**.

(32) Allen, F. H.; Kennard, O. *Chem. Des. Automat. News* **1993**, *8*, 31−37.

(33) (a) Delaigue, X.; Hosseini, M. W.; De Cian, A.; Fischer, J.; Leize, E.; Kieffer, S.; Van Dorsselaer, A. *Tetrahedron Lett.* **1993**, *34*, 3285−3288. (b) Juneja, R. K.; Robinson, K. D.; Johnson, C. P.; Atwood, J. L. *J. Am. Chem. Soc.* **1993**, *115*, 3818−3819.

Table 3. Results of Vacuum Calculations of 2b (kcal mol^{-1}) at T = 243 K

								Boltzmann(%)[e]			
conf[a]	E_{min}[b]	ΔA_{QM}	ΔA_{cl}	ΔA_0	σ[c]	ΔA_{rot}	n[d]	min	QM	clas	exp[f]
0000∼AAAA	3.8	−3.1	−4.1	−1.5	2	0.3	4	0.0	1.8	0.9	
0000∼AABA	5.1	−0.7	−0.9	−0.2	1	0.0	8	0.0	0.0	0.0	
0000∼ABAB	7.4	0.1	0.2	0.3	2	0.3	4	0.0	0.0	0.0	
0000∼AABB	15.1	0.8	1.5	1.3	1	0.0	8	0.0	0.0	0.0	
total cone								**0.0**	**1.8**	**0.9**	**4**
0001∼ABAA	0.0	0.0	0.0	0.0	1	0.0	8	51.5	1.1	1.9	
0001∼AAAA	1.1	−1.4	−2.0	−1.1	1	0.0	8	5.3	17.9	12.5	
0001∼AAAB	1.2	−2.2	−2.8	−0.9	1	−0.1	8	4.3	62.5	61.3	
0001∼ABAB	2.1	−0.7	−0.6	0.1	1	0.0	8	0.6	0.0	0.1	
0001∼BAAA	2.2	0.0	−0.0	0.1	1	0.0	16	1.2	0.0	0.0	
0001∼AABB	2.2	−0.7	−0.7	0.2	1	−0.1	16	1.1	0.1	0.2	
0001∼BABA	3.9	0.8	1.1	0.4	1	0.0	8	0.0	0.0	0.0	
0001∼BBAA	8.4	1.2	1.9	1.2	1	0.0	16	0.0	0.0	0.0	
0001∼BABB	8.5	−0.2	0.3	1.0	1	0.0	8	0.0	0.0	0.0	
0001∼ABBB	14.7	0.7	1.7	1.8	1	0.0	16	0.0	0.0	0.0	
total Paco								**64.0**	**81.7**	**76.0**	**85**
0011∼ABAB	0.7	−1.2	−1.2	0.0	1	−0.1	8	11.4	2.9	5.4	
0011∼AAAB	1.4	−1.1	−1.2	−0.2	1	−0.1	16	5.8	2.4	3.3	
0011∼ABBA	2.2	−0.9	−0.8	0.4	2	0.3	8	0.6	0.0	0.1	
0011∼AAAA	6.8	−2.2	−2.9	−1.2	1	−0.1	16	0.0	0.0	0.0	
0011∼BBBA	9.7	0.2	1.0	1.4	1	−0.1	16	0.0	0.0	0.0	
0011∼AABB	10.0	−0.1	0.4	1.1	1	−0.1	8	0.0	0.0	0.0	
total 1,2Alt									**5.3**	**8.8**	**8**
0101∼AAAA	0.5	−0.8	−1.3	−0.8	6	0.9	2	4.7	0.5	0.5	
0101∼AABA	0.8	−1.3	−1.7	−0.6	1	0.0	8	9.6	10.3	12.5	
0101∼AABB	1.3	−1.2	−1.4	0.0	2	0.3	8	3.4	0.5	1.3	
0101∼BABA	2.0	0.1	0.4	0.4	2	0.3	4	0.4	0.0	0.0	
0101∼ABBB	6.8	0.5	1.2	1.4	1	0.0	8	0.0	0.0	0.0	
0101∼BBBB	13.4	1.9	3.3	2.4	6	0.8	2	0.0	0.0	0.0	
total 1,3Alt								**18.0**	**11.2**	**14.3**	**3**

[a] The digits in the names of conformations indicate which anisole ring is inverted. The letters indicate whether the methoxy group attached to each aromatic ring points outward (A) or inward (B). For example: 0001∼AAAB is a Paco in which the methoxy group on the inverted aromatic ring points inward. [b] Minimized potential energy. [c] Rotational symmetry number. [d] Degeneracy of conformation. [e] min: calculated with only E_{min}; QM: calculated including ΔA_{QM}; clas: calculated including ΔA_{cl}. [f] Distribution in $CDCl_3$ at 243 K taken from ref 9.

these values are both negative, while in $CDCl_3$ they are both positive.

Vacuum Calculations. The methoxy moieties of **2** can point into the annulus of the calix[4]arene or point outward. In all published calculations in Table 1 except entry CHARMM22,[12] the conformational energies of **2b** were calculated using only one representative of every conformation, in most cases a conformation with all methoxy moieties pointing outward. The high-field position of some of the methoxy signals of **2b** in the $CDCl_3$ NMR spectrum indicates that the methoxy groups of the 1,2Alt and 1,3Alt, and one of the methoxy groups of the Paco, are at least part of the time pointing inward.[9] We therefore took all possible methoxy in/out conformations into account.

The calculation of the conformational distribution can in principle be improved by normal-mode analysis and calculation of the rotational free energy.[34] The results for compound **2b** are presented in Table 3. The maximum difference between the quantum mechanically and classically calculated normal mode contributions is in the order of 5% (absolute). Because of the small difference between the classically and quantum mechanically calculated vibrational free energies, we will focus on the quantum mechanical contribution from now on. The calculated conformational distribution for **2b**, including vibrational and rotational free energies, is correct within a few percent compared with the experimental distributions determined in $CDCl_3$ in Table 1. The largest difference is found for the 1,3Alt conformation, which is calculated to be more stable than found experimentally. The influence of the rotational contribution is small since it largely depends on the rotational symmetry number σ which is equal to 1 for most conformations with nonvanishing abundance. The normal mode contribution changes the calculated conformational distribution of **2b** drastically. The minimized energy of the lowest energy cone conformation (0000∼AAAA) is too high to contribute to the conformational distribution (the minimized energy is 3.8 kcal mol^{-1} higher than for the lowest energy conformation, 0001∼ABAA), but the free energy is lowered by 4.6 kcal mol^{-1} due to the normal mode contribution (Table 3). The 0000∼AAAA is the conformation with the most favorable vibrational contribution. Furthermore, the order of the three most stable Paco conformations is changed: the 0001∼AAAB conformation is now the most stable. The order of stabilities of the 1,2Alt and 1,3Alt conformations is not affected.

In comparison to energy minimization of the four main conformations, the following improvements to the calculated distribution have been applied: differentiation of methoxy in/out conformations, calculation of vibrational and rotational contributions, and inclusion of degeneracies of the conformations. The merits of these additions are discussed in our previous paper,[12] except for the calculation of the vibrational and rotational contributions. Only the stabilities of the conformers 0000∼AAAA and 0101∼AAAA are affected by the rotational contribution, because these are the only low-energy conformations with $\sigma \neq 1$. When the rotational contribution is ne-

(34) Burkert, U.; Allinger, N. L. *Molecular Mechanics*; American Chemical Society: Washington, DC, 1982.

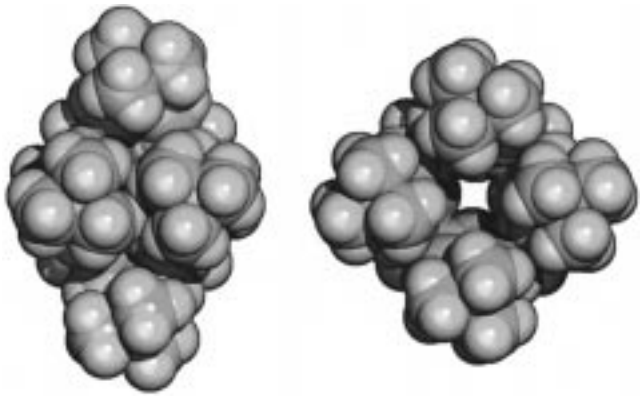

Figure 2. Spacefilling representations of the "pinched" or "flattened" C_{2v} cone (left) and the "perfect" C_{4v} cone (right) of **2b**.

glected, the conformational distribution of **2b** changes maximally 5% (absolute). Thus, if the rotational symmetry numbers σ differ from 1, the rotational contribution has a small but significant effect on the Boltzmann distribution and hence cannot be neglected.

The vibrational contribution changes the order of the three most stable Paco conformations of **2b**: the 0001~AAAB conformation is now the most stable. This conformation is most likely the conformation observed in chloroform solution, based on the high-field position in the ^{1}H NMR spectrum (δ = 1.99 ppm) of one methoxy group.[9,12] The second most stable Paco conformation, 0001~AAAA, is the conformation found in the solid state.[9] The conformation which was most stable after minimization alone, 0001~ABAA, is calculated to be present in minute quantities (0.3%). The position of the methoxy moiety opposite to the flipped aromatic ring in the ^{1}H NMR spectrum (δ = 3.46 ppm) does not indicate that this methoxy group is pointing inward, thus the low abundance of this conformation is in accordance with the NMR data.

The vibrational contribution changes the conformational distribution of **2b** drastically, and it brings the calculated distribution in better accordance with experimental data in chloroform. The difference between the vibrational contribution calculated quantum mechanically and classically is maximally 5%.

Liquid-Phase Calculations. When comparing the experimental conformational distributions of **2b** in chloroform and dichloromethane, the cone/Paco ratio differs most, while the relative stabilities of the 1,2Alt and 1,3Alt are less affected. We decided to perform MD calculations in order to get insight into the stabilization by the solvent of the cone and Paco conformations of **2b**. Moreover, MD simulations offer a method to sample the anharmonic degrees of freedom, while normal-mode analysis only samples harmonic degrees.

Simulations of the Cone. First, the inclusion behavior of dichloromethane and chloroform molecules in the cavity of the cone of **2b** has been investigated. The energy-minimized 0000~AAAA conformation of **2b** has C_{2v} symmetry (pinched cone), in which the planes of two opposite aromatic rings are almost parallel to each other, and the other two rings are tilted away from the annulus. In this conformation the cavity is blocked by the *tert*-butyl moieties (Figure 2). The C_{4v} cone (perfect cone) has been calculated to be the transition state when going from one C_{2v} cone to the other in a vacuum.[12] The four aromatic rings are tilted away equally from the annulus, giving the perfect cone a distinct cavity. This conformation can be stabilized by an included solvent molecule as shown by X-ray diffraction.[18] Therefore, we took this conformation to investigate solvent inclusion. For both solvents, two different calix[4]arene−solvent complexes, one with a Cl atom and one with a CH_x atom in the cavity, were energy minimized in a vacuum. After minimization, both complexes of **2b** with dichloromethane had the same conformation in which the CH_2 points into the cavity. We therefore neglected the starting conformation with the Cl pointing into the cavity. The minimized complexes of **2b** were submerged into a solvent box containing the same solvent molecules as the one in the cavity, and three MD simulations of 500 ps were performed. The solvation of calix[4]arenes in the cone conformation has further been investigated by performing two 500 ps MD simulations in chloroform and dichloromethane, without initially included solvent molecules.

We assigned symbolic names to these simulations: *CN_y_z*, in which *CN* indicates the cone, *y* the solvent ($CHCl_3$ or CH_2Cl_2) and *z* the starting configuration (0 for empty cavity, or atom which points into the cavity for simulations with an included solvent). The five MD simulations performed bear the following names:

CN_CHCl$_3$_Cl: Cone in chloroform starting with one $CHCl_3$ molecule pointing with a Cl atom into the cavity.

CN_CHCl$_3$_CH: Cone in chloroform starting with one $CHCl_3$ molecule pointing with the CH atom into the cavity.

CN_CHCl$_3$_0: Cone in chloroform starting with an empty cavity.

CN_CH$_2$Cl$_2$_CH$_2$: Cone in dichloromethane starting with one CH_2Cl_2 molecule pointing with the CH_2 atom into the cavity.

CN_CH$_2$Cl$_2$_0: Cone in dichloromethane starting with an empty cavity.

When visually inspecting, no differences could be observed between the two simulations of **2b** with chloroform in the cavity (*CN_CHCl$_3$_CH* and *CN_CHCl$_3$_Cl*). During both simulations, the included solvent molecule was not in a fixed orientation, but translated and rotated considerably in the cavity. Both possible extreme configurations of chloroform inclusion, Cl or CH pointing into the cavity, were found during both simulations (Figure 3a,b). The inclusion of a chloroform molecule in the cavity of **2b** is not stable, since the included solvent molecule leaves the cavity during both the simulations (after ≈315 and ≈250 ps for *CN_CHCl$_3$_CH* and *CN_CHCl$_3$_Cl*, respectively). The remaining parts of these simulations behaved as simulation *CN_CHCl$_3$_0*, during which the cavity of **2b** remained empty. In contrast to the chloroform simulations of **2b**, the included dichloromethane molecule remains in the same position during the entire simulation *CN_CH$_2$Cl$_2$_CH$_2$* (Figure 3c). The CH_2 atom is pointing into the cavity, and almost no rotation takes place around the axis connecting the CH_2 atom and the mean of the two chloro atoms. The inclusion of a dichloromethane molecule in **2b** is so stable that one of the bulk dichloromethane molecules diffuses into the cavity of **2b** during the simulation *CN_CH$_2$Cl$_2$_0* (between 100 and 105 ps) and remains there for the remaining 400 ps in the same position as during simulation *CN_CH$_2$Cl$_2$_CH$_2$*. Thus of the five simulations in-

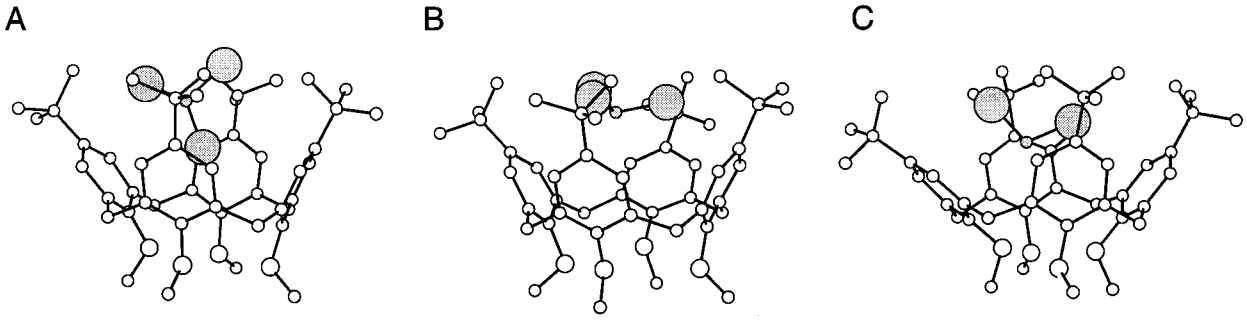

Figure 3. Typical snapshots from the cone simulations of **2b**. (a) *CN_CHCl3_xx* with Cl inside configuration. (b) *CN_CHCl3_xx* with CH inside configuration. (c) *CN_CH2Cl2_CH2* with CH_2 inside configuration.

Table 4. Average Properties from MD Simulations of 2b[a]

simulation	E_{int} calix-solv:	vdW/elec	E_{conf} calix[b]	E_{conf} solvent	E_{int} included
		Simulations in $CHCl_3$			
CN_CHCl3_CH[c]	−90.7 (4.9):	−85.2/−5.5	103.2 (6.8)	−1163 (14.9)	−11.9 (1.8)
CN_CHCl3_Cl[d]	−90.5 (4.6):	−85.8/−4.8	104.1 (5.7)	−1217 (15.5)	−11.3 (1.9)
CN_CHCl3_0	−79.7 (4.4):	−75.2/−4.5	95.8 (6.5)	−1198 (16.5)	
PC~AAAA_CHCl3	−79.1 (4.3):	−74.8/−4.3	98.2 (6.8)	−1175 (15.4)	
PC~AAAB_CHCl3	−84.0 (4.6):	−77.2/−6.8	93.1 (6.7)	−1151 (15.6)	
		Simulations in CH_2Cl_2			
CN_CH2Cl2_CH2	−99.3 (4.9):	−79.6/−19.7	100.6 (7.0)	−1330 (14.3)	−17.7 (1.6)
CN_CH2Cl2_0[e]	−88.9 (5.3):	−71.9/−17.0	100.0 (5.6)	−1366 (13.3)	
PC~AAAA_CH2Cl2	−82.5 (5.2):	−71.3/−11.2	91.7 (6.5)	−1359 (14.0)	
PC~AAAB_CH2Cl2	−90.6 (6.3):	−72.4/−18.1	95.4 (6.6)	−1360 (14.5)	

[a] Energies in kcal mol^{-1}, in brackets: standard deviation. Averages are taken over 500 ps. [b] Relative to minimized energy of 0001~AAAA conformation. [c] Average first 250 ps. [d] Average first 200 ps. [e] Average first 100 ps.

volving calix[4]arene **2b**, only the simulations *CN_CH2Cl2_CH2* and *CN_CHCl3_0* are stable.

The nonbonded interactions (electrostatic and van der Waals) between the cone conformations of **2b** and the solvent have been determined for every frame of the simulations, and the averages are presented in Table 4. While the chloroform is still included in the cavity during *CN_CHCl3_CH* and *CN_CHCl3_Cl*, the average total solvent/solute interaction is −10.9 kcal mol^{-1} more favorable than during *CN_CHCl3_0*. This improved interaction is almost completely caused by a better van der Waals interaction of −10.3 kcal mol^{-1}. The more favorable solvent/solute interaction is completely due to the interaction of **2b** with the included chloroform molecule which amounts to −11.6 kcal mol^{-1}. It is, however, opposed by a 7.9 kcal mol^{-1} higher potential energy of **2b** itself during chloroform inclusion. The net result of chloroform inclusion becomes then a favorable −3.0 kcal mol^{-1}. We consider this number an estimation of $\Delta H_{complexation}$ of the following equilibrium:[35]

$$\text{cone} + CHCl_3 \rightleftarrows (\text{deformed cone})\cdot CHCl_3 \qquad (8)$$

The fact that during both simulations *CN_CHCl3_CH* and *CN_CHCl3_Cl* the included chloroform molecule spontaneously leaves the cavity of **2b** indicates that the equilibrium is shifted to the left, which leads to $\Delta G_{complexation} > 0$. With $\Delta H_{complexation} = -3.0$ kcal mol^{-1}, $T\Delta S_{complexation}$ can be estimated < −3.0 kcal mol^{-1}. Thus the decrease in rotational and translational freedom upon inclusion of a chloroform molecule in **2b** makes complexation unfavorable.

(35) The energy contribution of solvent restructuring is left out because this number shows a very large standard deviation for all simulations (≈15 kcal mol^{-1}, see Table 4).

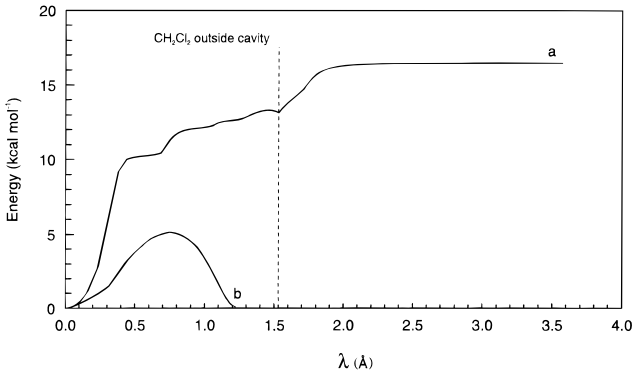

Figure 4. Energy profile of a dichloromethane molecule leaving the cavity of **2b** (a) and of the C_{2v}/C_{2v} interconversion of **2b** with an included dichloromethane molecule (b).

During simulation of **2b** with an included dichloromethane molecule, *CN_CH2Cl2_CH2*, the average total solvent/solute interaction is −10.4 kcal mol^{-1} more favorable than during the first 100 ps of *CN_CH2Cl2_0* (where no dichloromethane has yet diffused into the cavity). This more favorable interaction is mainly caused by a more favorable van der Waals interaction (−7.6 kcal mol^{-1}, compared to the electrostatic interaction of −2.7 kcal mol^{-1}). The interaction between **2b** and the included dichloromethane molecule amounts to −17.7 kcal mol^{-1}, so the total gain of solvent/solute interaction is 7.3 kcal mol^{-1} less than the gain of including dichloromethane in the cavity. The potential energy of **2b** is only 0.6 kcal mol^{-1} higher upon dichloromethane inclusion. The net result of dichloromethane inclusion becomes then a favorable −9.8 kcal mol^{-1}. We consider this number as an estimation of $\Delta H_{complexation}$ of the following equilibrium:[35]

$$\text{cone} + CH_2Cl_2 \rightleftarrows (\text{deformed cone})\cdot CH_2Cl_2 \qquad (9)$$

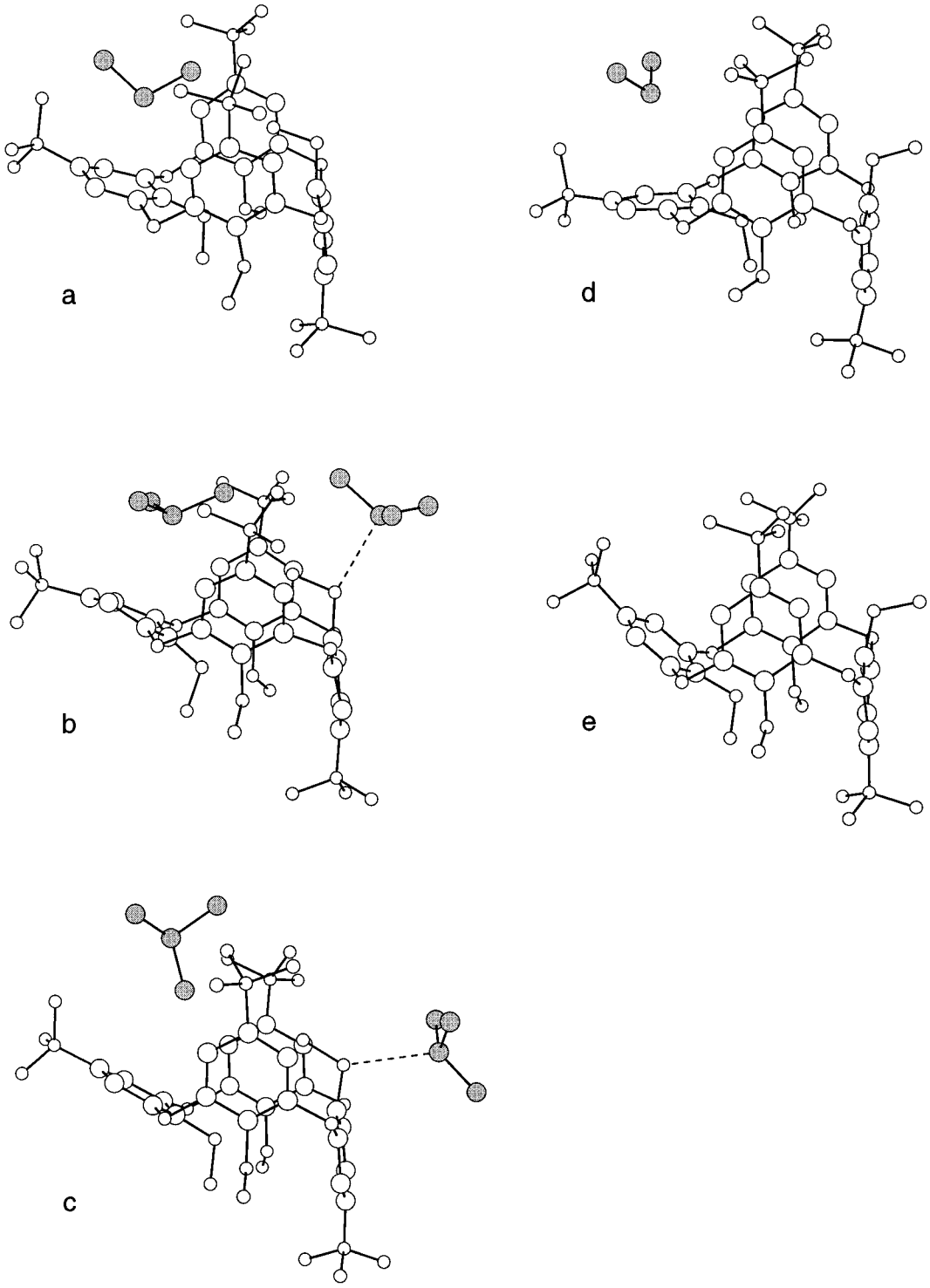

Figure 5. Snapshots from the Paco simulations of **2b**: *PC*_AAAB_CH_2Cl_2 (a), *PC*_AAAB_$CHCl_3$ (b,c), *PC*_AAAA_CH_2Cl_2 (d), and *PC*_AAAA_$CHCl_3$ (e).

This equilibrium is shifted to the right, which leads to $\Delta G_{complexation} < 0$. With $\Delta H_{complexation} = -9.8$ kcal mol^{-1}, $T\Delta S_{complexation}$ can be estimated > -9.8 kcal mol^{-1}. Because of the loss of translational and rotational degrees of freedom upon complexation, the entropy decreases, so that $-9.8 < T\Delta S_{complexation} < 0$ kcal mol^{-1}.

The spontaneous inclusion of a dichloromethane molecule within the first 105 ps of an MD simulation suggests that this process has a low activation barrier. This is confirmed by calculating the reaction path of the included dichloromethane molecule leaving the cavity. The reaction path was calculated with travel which yields a string of conformations along the reaction coordinate. The starting point of the calculation was the energy-minimized complex of **2b** with included dichloromethane, and the final point the energy-minimized 0000∼AAAA conformation from Table 3, with the dichloromethane molecule at a distance of 20 Å. The energy profile of the reaction is shown in Figure 4a. The energy along the reaction coordinate increases gradually, with no transition state. When the dichloromethane has just left the cavity (at $\lambda = 1.5$ Å), the energy has increased ≈13 kcal

mol^{-1}. The energy plateau at a large calixarene−dichloromethane distance amounts to ≈16.5 kcal mol^{-1}, which is in close agreement of the average calculated from the MD simulations of 17.7 kcal mol^{-1}.

The cone of **2b** measured with NMR shows C_{4v} symmetry, while the lowest energy 0000∼AAAA conformation and most X-ray conformations of tetrafunctionalized calix[4]arenes have C_{2v} symmetry (Figure 2).[9,11] This has been explained by rapid (on the NMR time scale) interconversion of two equivalent C_{2v} conformers.[6,12] To rule out the possibility that this included solvent molecule blocks the C_{2v}/C_{2v} interconversion, we calculated with travel the reaction pathway of the C_{2v}/C_{2v} interconversion with an included dichloromethane (Figure Figure 4). The calculated energy barrier is 5.1 kcal mol^{-1}, only 2.0 kcal mol^{-1} higher than the previously[12] calculated reaction pathway of C_{2v}/C_{2v} interconversion without a solvent molecule in the cavity. The barrier with included solvent is low enough to be in accordance with a fast C_{2v}/C_{2v} interconversion on the NMR time scale.

Simulations of the Paco. For **2b**, 0001∼AAAA and 0001∼AAAB are the most stable Paco conformers. To investigate the solvation of the Paco relative to the cone, MD simulations of both Paco conformers have been performed in both chloroform and dichloromethane. The four 500 ps Paco simulations bear symbolic names analogous to the cone simulations: *PC_y_z*, in which *PC* indicates the Paco, *y* the orientation of the methoxy moieties (AAAA or AAAB), and *z* the solvent ($CHCl_3$ or CH_2Cl_2):

PC∼AAAA_$CHCl_3$: 0001∼AAAA in chloroform.

PC∼AAAA_CH_2Cl_2 : 0001∼AAAA in dichloromethane.

PC∼AAAB_$CHCl_3$: 0001∼AAAB in chloroform.

PC∼AAAB_CH_2Cl_2 : 0001∼AAAB in dichloromethane.

No change of the in/out orientation of any methoxy moiety was observed during the Paco simulations. During *PC*∼AAAB_CH_2Cl_2, a dichloromethane molecule entered the cavity of the Paco twice for a period of ≈20 ps (Figure 5a), but for the rest of the simulation the cavity remained empty. The dichloromethane molecule was not tightly immobilized, but moved around considerably. It was found almost exclusively with the CH_2 atom pointing into the cavity. When the same Paco conformation was simulated in chloroform (*PC*∼AAAB_$CHCl_3$), a configuration with one chloroform molecule in the cavity of the Paco was found several times, but on the complete timespan of the simulation inclusion was rare. Both the chloro and the CH atoms were found pointing into the cavity (Figure 5b,c). Almost throughout the entire simulation, one chloroform molecule was observed in the vicinity of the oxygen atom of the inverted aromatic ring with the CH atom pointing toward the oxygen, forming a CH··O hydrogen bond. This chloroform molecule exchanged multiple times with a bulk solvent molecule. This arrangement was also observed during the dichloromethane simulation *PC*∼AAAB_CH_2Cl_2, but less frequently and with a larger CH_2−O distance. For 0001∼AAAA, no hydrogen bonds were observed during simulations in either solvent. In this conformer, the methyl group of the inverted aromatic ring shields the oxygen atom from the solvent. Solvent inclusion was observed during simulation *PC*∼AAAA_CH_2Cl_2, and inclusion occurred most frequently of all Paco simulations. But also in this simulation the cavity was empty most of the time. The aromatic ring opposite to the inverted ring is in the most outward position of all Paco simulations, especially when a dichloromethane molecule is in the cavity (Figure 5d). No solvent inclusion was observed during *PC*∼AAAA_$CHCl_3$.

The inclusion of solvent molecules is possible for both Paco conformers, while it was expected that the methyl group on the inverted ring of 0001∼AAAB would at least partly fill the cavity, thus hampering inclusion. However, the two parallel aromatic rings of 0001∼AAAA are closer to each other than the rings of 0001∼AAAB. In the latter conformation, the included methyl group pushes the rings apart and enlarges the cavity. This is illustrated by the across cavity C^{para}−C^{para} distances (C^{para} is the atom to which the R group is attached in Chart 1): 5.4 and 7.0 Å for the energy minimized 0001∼AAAA and 0001∼AAAB conformers, respectively.

The average energies of the Paco simulations are presented in Table 4. In chloroform, the CH··O hydrogen bond is the cause for the better solvation of 0001∼AAAB compared to 0001∼AAAA. The average interaction[36] of this chloroform molecule with **2b** is −6.3 kcal mol^{-1}, while of the included molecule it is −7.1 kcal mol^{-1}. But inclusion is occurring rarely and has not a large effect on the overall interaction energies. The average conformational energy of 0001∼AAAB is 5.1 kcal mol^{-1} more favorable than of 0001∼AAAA, which was also observed by the normal mode calculations. The better solvation and lower conformational energy favor 0001∼AAAB over 0001∼AAAA by 10.0 kcal mol^{-1}. The entropically unfavorable hydrogen bond between 0001∼AAAB and chloroform will lower this number, but based on the MD calculations we predict that 0001∼AAAB is the most stable Paco conformer, in accordance with NMR results[9] and normal mode calculations. In dichloromethane, the order of the conformational energies of the Paco conformers is reversed compared to chloroform. The 0001∼AAAA is favored by 3.7 kcal mol^{-1} over 0001∼AAAB. But like in chloroform, the 0001∼AAAB conformer has a more favorable interaction with the solvent (8.1 kcal mol^{-1}), rendering it the most favorable Paco conformer by 4.4 kcal mol^{-1}, in accordance with NMR results.

When assuming 0001∼AAAB as the only Paco conformer in both solvents, and an included solvent molecule for the cone in dichloromethane, the following equilibria are measured with NMR:[35]

$$\begin{aligned} &CHCl_3:\ 0001{\sim}AAAB{\cdot\cdot}CHCl_3 \rightleftarrows \text{cone} \\ &CH_2Cl_2:\ 0001{\sim}AAAB + CH_2Cl_2 \rightleftarrows \\ &\qquad\qquad (\text{deformed cone}){\cdot}CH_2Cl_2 \end{aligned} \tag{10}$$

In chloroform, the measured ΔH for the Paco/cone equilibrium is expected to be positive because the sum of the conformational energy of the conformer plus the solvent interaction is more favorable for 0001∼AAAB than for the cone (by 7.0 kcal mol^{-1}). The CH··O hydrogen bond of 0001∼AAAB is lost in the cone, which is entropically favorable. Therefore, we expect a positive ΔS. In dichloromethane this reasoning is reversed. The sum of the conformational energy of the conformer plus the solvent interaction favors the cone over 0001∼AAAB (by 3.5 kcal mol^{-1}), and a negative ΔH is expected. An entropically unfavorable complex in formed in the cone,

(36) This average interaction was calculated by averaging over multiple chloroform−**2b** hydrogen bond pairs.

which leads to a negative ΔS. This qualitative discussion is in full agreement with the NMR results in Table 2.

The cone has a larger dipole than the Paco[17] and dichloromethane is a more polar solvent than chloroform; thus we expected the largest electrostatic interaction for the cone in dichloromethane. This is indeed found, but only because a dichloromethane molecule is included in the cone. When the empty cone simulations are compared to the Paco simulations, the largest electrostatic interaction is found for 0001∼AAAB, and this is more pronounced in chloroform than in dichloromethane. These results indicate that it can be dangerous to explain stabilities of conformers by solely looking at the dipole moments of the conformers and the polarity of the solvents, especially when solvent inclusion or hydrogen bonding are possible.

Conclusions

Energy minimization is widely used to discriminate between different conformers of a molecule.[6−12,37] The present study shows that the methodology of vacuum calculations can significantly be improved by calculating the rotational and vibrational free energies. Molecular dynamics simulations show that the cavity of the cone of **2b** contains a solvent molecule in dichloromethane, but not in chloroform. The inclusion of a chloroform molecule is favorable energetically, but not stable because of the unfavorable entropy of complex formation. In both chloroform and dichloromethane, the 0001∼AAAB conformer is the most stable Paco (in this conformation the methoxy moiety connected to the inverted aromatic ring is pointing into the cavity of **2b**). The stability of this conformer is due to the possibility of CH··O hydrogen bonds. This study shows that even low-dielectric solvents can have a significant influence on the stability of conformers.[38] This solvent effect is enhanced if a solvent molecule can be bound into a cavity,[2,39,40] or if hydrogen bond formation is possible. "Magic" attractive interactions[40] like CH_3··π interactions[19] or "Lewis bonding" interactions,[37] postulated in the literature to explain the difference between calculated and experimental stability of conformations may be attributed to solvent effects.

JO972134+

(37) Sakakibara, K.; Allinger, N. L. *J. Org. Chem.* **1995**, *60*, 4044−4050.

(38) Jorgensen, W. L.; McDonald, N. A.; Selmi, M.; Rablen, P. R. *J. Am. Chem. Soc.* **1995**, *117*, 11809−11810.

(39) Chin, D. H.; Gordon, D. M.; Whitesides, G. M. *J. Am. Chem. Soc.* **1994**, *116*, 12033−12044.

(40) (a) Chapman, K. T.; Still, W. C. *J. Am. Chem. Soc.* **1989**, *111*, 3075−3077. (b) Blake, J. F.; Jorgensen, W. L. *J. Am. Chem. Soc.* **1990**, *112*, 7269−7278. (c) Chapman, R. G.; Chopra, N.; Cochien, E. D.; Sherman, J. C. *J. Am. Chem. Soc.* **1994**, *116*, 369−370. (d) Whitlock, B. J.; Whitlock, H. W. *J. Am. Chem. Soc.* **1994**, *116*, 2301−2311.